

by multiple scattering into alignment in the planar regions. At this optimum incidence angle one expects the yields of all close interactions to reach maxima. This is a prediction of our model which can be easily tested experimentally.

In the above discussion we have considered two extreme anisotropic effects: channeling and blocking. A complete description of all intermediate situations where a particle trajectory may go from one to the other and also to become random in parts of its path through the crystal is beyond analytical calculations. This may be best achieved by machine calculations, possibly on the basis of the approximations we have made: use of effective potentials for channeling ($\rho > a$) and effective atomic densities for blocking ($\rho < a$). In both extremes, as in the intermediate situations, the physical process responsible for anisotropy is the same: multiple Coulomb scattering in a crystalline medium that exhibits a high degree of atomic and electronic heterogeneity only to those particles making small angles with the symmetry arrays.

I acknowledge with thanks many discussions with W. M. Gibson, H. E. Wegner, and B. R. Appleton on the experiments, and with G. H. Vineyard and M. W. Thompson on the theory of channeling.

Note added in proof.—After this manuscript was submitted, a preprint by J. Lindhard was received, in which directional effects are treated in great detail but somewhat differently,

especially as regards planar effects.

*Work performed under the auspices of the U. S. Atomic Energy Commission.

¹R. S. Nelson and M. W. Thompson, *Phil. Mag.* **8**, 1677 (1963); see also erratum in *Phil. Mag.* **9**, 1069 (1964).

²G. Dearnaley, *IEEE, Trans. Nucl. Sci.* **11**, 243 (1964).

³C. Erginsoy, H. E. Wegner, and W. M. Gibson, *Phys. Rev. Letters* **13**, 530 (1964).

⁴E. Bogh, J. A. Davies, and K. O. Nielsen, *Phys. Letters* **12**, 129 (1964).

⁵M. W. Thompson, *Phys. Rev. Letters* **13**, 756 (1964).

⁶W. Brandt, J. M. Khan, D. L. Potter, R. D. Worley, and H. P. Smith, *Phys. Rev. Letters* **14**, 42 (1965).

⁷B. Domeij and K. Bjorkqvist, *Phys. Letters* **14**, 127 (1965).

⁸G. Astner, I. Bergstrom, B. Domeij, L. Eriksson, and Å. Persson, *Phys. Letters* **14**, 308 (1965).

⁹D. S. Gemmell and R. E. Holland, *Phys. Rev. Letters* **14**, 945 (1965).

¹⁰J. Lindhard, *Phys. Letters* **12**, 126 (1964).

¹¹W. M. Gibson, C. Erginsoy, H. E. Wegner, and B. R. Appleton, (preceding Letter) [*Phys. Rev. Letters* **15**, 357 (1965)].

¹²A. R. Sattler and G. Dearnaley, to be published.

¹³W. M. Gibson, C. Erginsoy, and H. E. Wegner, *Bull. Am. Phys. Soc.* **10**, 43 (1965).

¹⁴J. P. Schiffer and R. E. Holland, *Bull. Am. Phys. Soc.* **10**, 54 (1965).

¹⁵C. D. Moak and S. Datz, private communication.

¹⁶C. Lehmann and G. Leibfried, *J. Appl. Phys.* **34**, 2821 (1963).

¹⁷The temperature-dependent factor $\exp(\bar{u}_1^2/2\alpha)^2$ turns out to be the same as that in the formula for the energy loss of a focused collision chain with a Born-Mayer type of interatomic potential. For this see J. B. Sanders and J. M. Flint, *Physica* **30**, 129 (1964).

ROTATION AND ATTENUATION OF SHEAR SOUND WAVES IN COPPER*

J. D. Gavenda and J. R. Boyd†

The University of Texas, Austin, Texas

(Received 30 July 1965)

Recently there has been renewed interest in measuring the absorption edge first predicted by Kjeldaas¹ for circularly polarized ultrasonic waves in metals propagating parallel to a magnetic field \vec{B} . This interest arises from the fact that the location and shape of the edge are related to the shape of the Fermi surface expressed as a function of k_z , the component of electron wave vector parallel to \vec{B} . Thus a method is available for studying the properties of Fermi surfaces along \vec{B} , whereas most other techniques determine prop-

erties perpendicular to \vec{B} . In particular, it has been suggested² that one might test for the existence of a band gap caused by spin-density waves in potassium by examining the shape of this absorption edge.

Because of the severe experimental problems inherent in the generation of circularly polarized sound, all of the work on this effect to date has made use of linearly polarized shear sound waves.³⁻⁵ Since the velocities of right- and left-circularly polarized waves are slightly different functions of magnetic field, a lin-

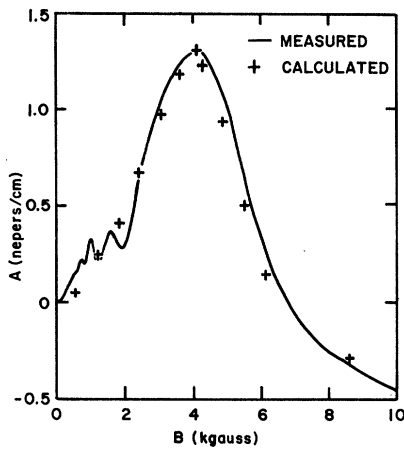


FIG. 1. Attenuation of 110-Mc/sec shear waves in copper as a function of external magnetic field, where $\vec{B} \parallel \vec{q} \parallel [001]$. The calculated points were obtained by the technique discussed in the text.

early polarized shear wave (which may be regarded as a linear combination of two circularly polarized waves) will exhibit a rotation of its plane of polarization which will also be a function of \vec{B} . The usual procedure of comparing the received pulse amplitude at a given field with that for zero field must be corrected for the variation in sensitivity of the receiving transducer as the plane of polarization rotates with respect to the polarization of the transducer. Since all previously reported work was done in metals with very complicated Fermi surfaces and the rotation of the polarization was not taken into account,⁶ there is not yet any clear-cut evidence for the existence of Kjeldaas absorption edges.

We report here measurements of the absorption "edge" in a pure single crystal of copper,⁷ a metal whose Fermi surface is relatively simple and well known. Actually, as shown in Fig. 1, a resonant peak in the attenuation is a more prominent feature than an "edge." The true attenuation A and the angle Φ through which the plane of polarization has rotated were obtained by measuring the apparent attenuations $\alpha(\vec{B})$ and $\alpha(-\vec{B})$ for \vec{B} parallel and antiparallel to \vec{q} , the sound-wave vector, and assuming that $\Phi(\vec{B}) = -\Phi(-\vec{B})$. Then, using these two sets of data along with the known angle between the polarizations of the transmitting and receiving transducers, we solved for A and Φ . As can be seen in Fig. 2, both A and Φ are periodic functions of ν/B , where ν is the sound frequency, although the period of Φ is twice

that of A . The amplitudes of the subharmonic peaks decrease with decreasing frequency. We will ignore them for the moment and examine the behavior of the main peak.

The general shape of the curve can be interpreted by assuming that only those electrons which move in phase with the sound wave contribute appreciably to the attenuation. This requirement will be satisfied for a band of electrons for which the condition

$$q\bar{v}_z(k_z) = \omega_c(k_z) \pm \omega \tag{1}$$

is satisfied, where \bar{v}_z is the average velocity of these electrons along \vec{q} , ω_c is the cyclotron frequency of the electrons, and $\omega = 2\pi\nu$. This condition is just that for a Doppler-shifted cyclotron resonance. As B (and therefore ω_c) increases, electrons with larger values of \bar{v}_z are effective. Eventually ω_c becomes so large that there are no electrons with \bar{v}_z satisfying (1). This defines the absorption edge.

Since $2\pi m_c \bar{v}_z = -\hbar(\partial S/\partial k_z)$, where S is the cross-sectional area of the Fermi surface perpendicular to \vec{B} and m_c is the cyclotron mass, Eq. (1) can be written in the form

$$B(k_z) = -(\hbar qc/2\pi e)(\partial S/\partial k_z). \tag{2}$$

Here ω has been neglected in comparison with ω_c . We can estimate the attenuation coefficient as a function of B by assuming that the energy

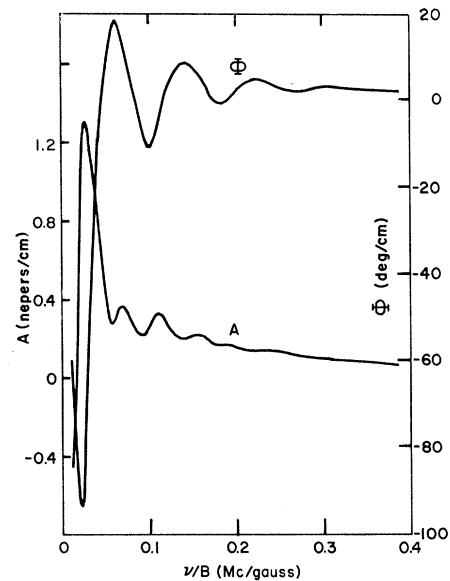


FIG. 2. Attenuation A and rotation of the plane of polarization Φ of 110-Mc/sec shear waves in copper as a function of ν/B , where ν is the frequency.

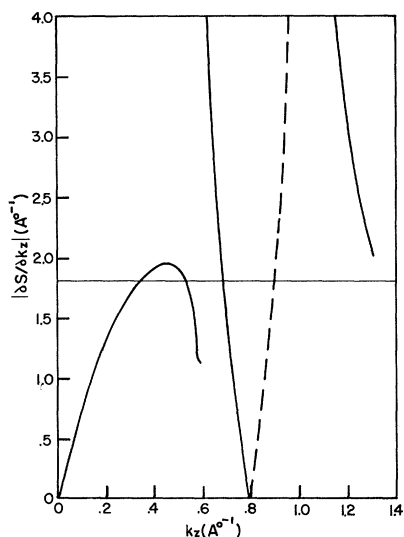


FIG. 3. $|\partial S/\partial k_z|$ along [001] in copper, where S is the cross-sectional area of the Fermi surface perpendicular to k_z . The curve is dashed where $\partial S/\partial k_z > 0$. The horizontal line indicates the portion of the surface effective for $B = 4.3$ kG, the field for which the large peak in attenuation occurs in Fig. 1.

absorbed by a band of electrons at k_z is proportional to the density of states at k_z :

$$dA \propto m_c(k_z) s(k_z) dk_z, \quad (3)$$

where $s(k_z)$ is the surface area of the band.

Figure 3, derived from Roaf's⁸ empirical Fermi surface for copper, shows the values of $|\partial S/\partial k_z|$ (and thus B) for which electrons having different values of k_z will satisfy (1) and therefore absorb energy from the sound field. The existence of a broad maximum at $k_z = 0.43 \text{ \AA}^{-1}$ means that a relatively large fraction of the Fermi surface will cause attenuation at the corresponding value of B computed from (2). This leads to the large peak observed at 4.2 kG in the experimental curve shown in Fig. 1. Several points computed by integrating (3) over bands of finite width (corresponding to finite $\omega_c\tau$, where τ is the electron relaxation time) for various values of B are also shown in Fig. 1 for comparison. The computed values of A have been scaled to correspond to the experimental value at the peak, but B is computed from Roaf's surface using (2) with the assumption that m_c has the free-electron value at $k_z = 0$.

The oscillatory features result from the large variation in v_z about the average \bar{v}_z for the dominant band. This band includes orbits pass-

ing over parts of the necks, so the real space orbits have a large oscillatory component along \vec{q} , as well as a drift velocity in this direction. Because of the fourfold symmetry of the copper Fermi surface about \vec{q} , the subharmonic resonances occur when electrons on the dominant band go one-fourth the distance around an orbit while moving one and one-fourth wavelengths along the sound wave, etc. The general condition for the attenuation resonances has been shown to be⁹

$$|4n \pm 1| + \Delta = |q\bar{v}_z/\omega_c|,$$

where $\Delta = 3^{-1/2}(\omega_c\tau)^{-1}$ and n is a non-negative integer. For the rotation curve one can show that maxima occur at $4n-1-\Delta = |q\bar{v}_z/\omega_c|$, where $n > 0$, and minima at $4n+1-\Delta = |q\bar{v}_z/\omega_c|$, where $n \geq 0$, so the spacing between maxima is twice that for attenuation maxima. Also, since the phase Δ of the peaks has opposite signs for A and Φ , careful measurements should give $\omega_c\tau$ for the dominant band.

It is clear from these results that great care must be exercised in analyzing ultrasonic data for Kjeldaas absorption edges in real metals. One should first plot A and Φ as functions of v/B to separate out subharmonics of the primary absorption peaks or edges. If $\omega_c\tau$ is not very large in a particular specimen, the Φ plot may prove more useful since it is more sensitive to small deviations of the Fermi surface from a free-electron surface.

A complete presentation of our experimental results will be published elsewhere, along with a development of the theory for oscillations in Φ for real metals.

We wish to acknowledge helpful discussions with Dr. L. M. Falicov concerning the relation of the attenuation to the shape of the Fermi surface. Most of the computer programs used in the reduction of the data and comparison with Roaf's surface were developed by Mr. D. B. Doan.

*Work supported by the National Science Foundation.

†Present address: The Center for the Study of Materials, Case Institute of Technology, Cleveland, Ohio.

¹T. Kjeldaas, Jr., Phys. Rev. **113**, 1473 (1959).

²R. C. Alig, J. J. Quinn, and S. Rodriguez, Phys. Rev. Letters **14**, 981 (1965).

³A. R. Machintosh, Phys. Rev. **131**, 2420 (1963).

⁴B. K. Jones, Phil Mag. **9**, 217 (1964).

⁵B. I. Miller, Bull. Am. Phys. Soc. **10**, 371 (1965).

⁶Miller (reference 5) used a pair of transducers

properly phased to detect circularly polarized components of shear waves in tin, but he was unable to relate the results to the Fermi surface because of its complexity.

⁷Same specimen used by B. C. Deaton and J. D.

Gavenda, Phys. Rev. 129, 1990 (1963).

⁸D. J. Roaf, Phil. Trans. Roy. Soc. A255, 135 (1962).

⁹E. A. Kaner, V. G. Peschanskii, and I. A. Privorotskii, Zh. Eksperim. i Teor. Fiz. 40, 214 (1961) [translation: Soviet Phys.-JETP 13, 147 (1961)].

TOTAL PHOTOPROTON CROSS SECTION AND BRANCHING RATIOS IN THE O¹⁶ GIANT RESONANCE*

R. C. Morrison, J. R. Stewart,† and J. S. O'Connell‡

Yale University, New Haven, Connecticut

(Received 19 July 1965)

In recent years, the O¹⁶(γ, n) total cross section has been measured with good resolution by Caldwell *et al.*¹ using monochromatic photons, and by Cook *et al.*² using bremsstrahlung yield-curve analysis. Yergin *et al.*³ have inferred neutron branching ratios for the decay of giant-resonance levels by comparing the spectrum of photoneutrons measured by time-of-flight techniques with the cross section for transitions to ground state measured by Geller and Muirhead.⁴ They reported branching to the 5.3-MeV positive-parity doublet in O¹⁵, from the O¹⁶ levels at 22.3 and 24.3 MeV, of 33 and 21%, respectively. However, this analysis has been disputed by Tanner and Earle⁵ and by a recent measurement of Caldwell *et al.*⁶

Up to the present time no comparable measurements of the oxygen photoproton cross section have been reported. The work reported here seeks to fill this gap. A "thin" target of O₂ gas, with natural isotopic content, was irradiated with bremsstrahlung produced by the Yale electron linac, with end-point energies of 22 and 40 MeV. A quadrupole triplet magnetic lens was used to transport the photoprotons, at 90° to the gamma beam, to a silicon detector two meters from the gas target. Absolute cross sections, with 80-keV energy resolution, were obtained by direct comparison of the photoproton yield from oxygen with the yield from deuterium, using the theoretical deuterium cross section of deSwart and Marshak.⁷ The experimental apparatus and technique have been described in detail in previous papers.^{8,9}

The threshold for proton transitions to excited states in N¹⁵ is 17.4 MeV. Thus with a bremsstrahlung end point of 22 MeV, all protons observed with energies greater than 4.6 MeV must result from ground-state transitions.

A proton spectrum was measured with 22-MeV bremsstrahlung over the proton energy range of 5 to 10 MeV, yielding a true ground-state cross section from $E_\gamma = 17$ to 22 MeV. A supplementary run with 24-MeV bremsstrahlung extended the range of this measurement to 23 MeV. The entire measurement was then re-

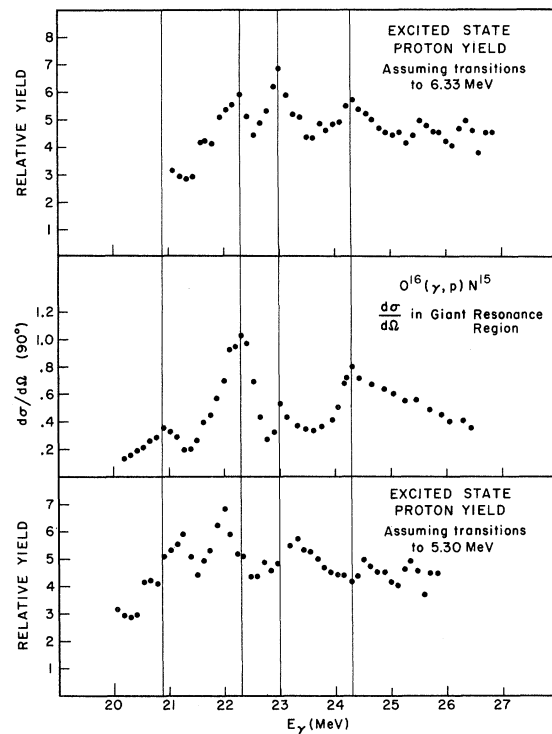


FIG. 1. A comparison between the proton spectrum from excited-state transitions and the giant-resonance ground-state cross section: In the upper portion of the figure, a gamma-energy scale has been assigned to the excited-state spectrum assuming all transitions are to 6.3 MeV. The lower portion shows the same spectrum assuming all transitions are to 5.3 MeV. The vertical lines are drawn through the cross-section peaks shown in the center portion of the figure.